Universitat Autònoma de Barcelona
Dep. Enginyeria Química
08193 Bellaterra, Barcelona, Spain

MELISSA

Memorandum of Understanding
ECT/FG/MMM/97.012

Contract Number: ESTEC/CONTRACT11549/95/NL/FG

TECHNICAL NOTE: 43.110

Characterisation of Hydrodynamic Behaviour of the Compartment IV Gas-lift Loop bioreactor.

Version: Draft
Issue: 0

VERNEREY A.; ALBIOL, J.; GODIA, F.

JULY 1997

Document Change Log

Version	Issue	Date	Observations
Draft	0	25/07/97	Preliminary Version
1	0	30/09/97	First revision

Table of Contents

I. INTRODUCTION

Implementation of the MELISSA loop will require the sizing of its components according to the amount of materials to recycle. This amount is directly proportional to the size of the crew for which the loop is designed. Appropriate development of the MELISSA loop requires an adequate scale up of its compartments in order to be able to evaluate the effect of the change of size of its components on its performance.

Compartment IV of the MELISSA loop is devoted to the culture *of Spirulina platensis* for CO_2 consumption, biomass production and oxygen regeneration. It was the first pilot bioreactor to be in operation with a volume of 7 litres. Reliable, highly automated and controlled operation of this bioreactor, has been achieved. A complete data set for the continuous operation has been generated along the last four years of operation. Scale-up of the bioreactor for compartment IV was recently performed to allow an increase of volume by a factor of ten from its previous size (Vernerey *et al.* 1996 (TN-25.2); Vernerey *et al.* 1998 (TN-37.2)).

As a guideline for the design of the scaled up bioreactor, it was considered convenient to maintain the previous type of reactor as far as possible, especially regarding model based predictive control. This way allows the efficient use of all the knowledge obtained in the previous unit. On the other hand, peripheral equipment and associated instrumentation was improved were necessary.

Accordingly, a 75 litres bioreactor of of the gas-lift type was chosen as the first concept to develope. Moreover, in order to improve one of the key design variables in a photobioreactor, namely the ratio of the volumes between the illuminated and the non illuminated part, it was considered that an gas-lift loop reactor (ALR) would represent an important improvement from the previous bioreactor design. This alternative type of bioreactor would allow to use the light transmission model developed in previous steps.

Some other design constraints had to be applied as well. The total height of the laboratory limited the total height of the bioreactor. For this reason, and also to maximize the illuminated to total volume ratio, an external loop gas-lift reactor was the final design adopted. The metallic part should be made in standard sizes so that not to increase the cost of the unit and the size of the illuminated part should be made of plastic foil for safety reasons.

Variable	Value
Illuminated tube diameter	0.15 m
Illuminated tube length	1.5 m (each)
Connecting sections diameter	0.12 m
Polyamide foil thickness	80 μm
Working total volume	77 l
Illuminated volume	53 l
Illuminated vol./working vol.	0.688
Total Illuminated area	1.41 m^2

Table 1: Main dimensions of the gas-lift loop bioreactor.

Once all the considerations were taken into account, the final design was built by the firm Bioengineering AG (Switzerland). A scheme of the final design can be seen in figure 1. Table 1summarizes the main dimensions of the external loop ALR. A gas loop was implemented in this bioreactor as shown in figure 2.

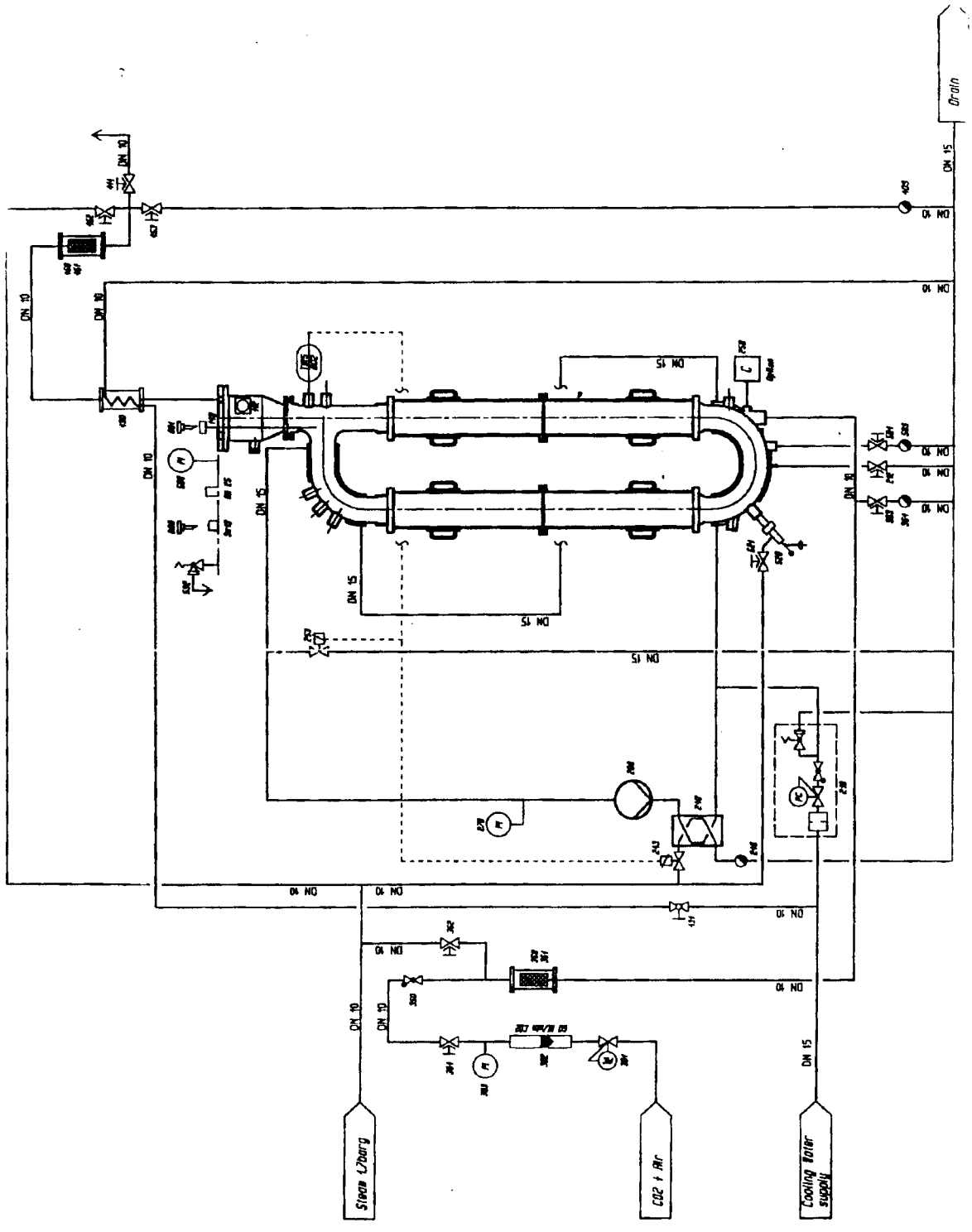

Figure 1: General overview of the gas-lift loop bioreactor.

Evaluation and modelling of the performance of a bioreactor, requires to accurately know the behaviour of the bioreactor. As main important points, the fluid dynamics and its influence on the degree of mixing and residence time behaviour, together with the gas-liquid mass transfer characteristics can be mentioned. These factors are well known in the case of 'ideal' bioreactors, however the behaviour of the 'real' bioreactors, differs from such idealised situations. The deviations might arise as a result of the existence of characteristic traits which result in the formation of local variations in the flow patterns such as dead zones, by-pass of input medium and others. All this has the net result of a decrease in the efficiency of that bioreactor performance.

When deviations of the ideal case are small, the behaviour of the bioreactor can be accurately described by the equations used for the ideal situations. In other cases, such deviations are high enough so as to require the use of different models. All those factors are influenced by the change of scale and require an evaluation for new bioreactor designs such as in the present case.

In the operation of a bioreactor it can be desirable to homogenize all components of a reaction system as rapidly and as uniformly as possible throughout the entire reaction volume. This is a desired characteristic for those reactors based on the concept of stirred tank. This allows to maintain a uniform solute and biomass concentrations as well as a uniform temperature in the bioreactor. The required mixing effect should be achieved with as low power input as possible.

There are special cases in which this homogeneity can not be attained, like in the case of light intensity were, even if the bioreactor is homogeneous, the light intensity measured in one point is different to the one in another point due to the effects of absorption and scattering. However, even in those special cases it is desirable to have a uniform biomass distribution, in order to be able to calculate the light intensity in different points of the bioreactor, knowing the light intensity in one point and the biomass concentration. In the case of illuminated bioreactors, adequate mixing is also required so as to assure that all the cells in the culture receive an averaged illumination as a result of their residence time in illuminated and non illuminated parts of the bioreactor.

Gas-lift loop reactors obtain their mixing by hydrostatic flow drive, caused by different densities of the fluid in communicated tubes, due to different gas hold up. Two fundamental mixing effects superimpose each other, namely the longitudinal mixing in each circulation and back-mixing due to recycling of the circulation flow. Longitudinal mixing is caused in each longitudinal tube mainly by the flow stream profile, turbulence and molecular diffusion. The combination of this two effects, result in a characteristic pattern of mixing which in practice, results in a characteristic mixing time. This one represents the time necessary to reach homogeneity after a certain input of a substance.

Experimental determination of the mixing time is usually done by introducing a pulse of a substance in the reactor in batch mode. Following the pulse, the change in concentration of the pulsed compound inside the bioreactor is recorded. The time evolution of this concentration gives information of the type of flow and mixing inside the bioreactor, and allows modelling it as well as determination of the mixing time.

In order to compare different situations, the mixing time is defined as the time required to reach a certain degree of mixing. For example, the time required to reach a concentration value within the +/-5% of the final concentration. The final concentration being the concentration of the pulsed compound when it is perfectly and completely mixed in the total volume.

The changes of tracer concentration with time, measured at one point of the external loop ALR, generates an oscillatory curve. The maxima reached by the curve at each oscillation can be connected by a decreasing curve named upper-envelope curve.

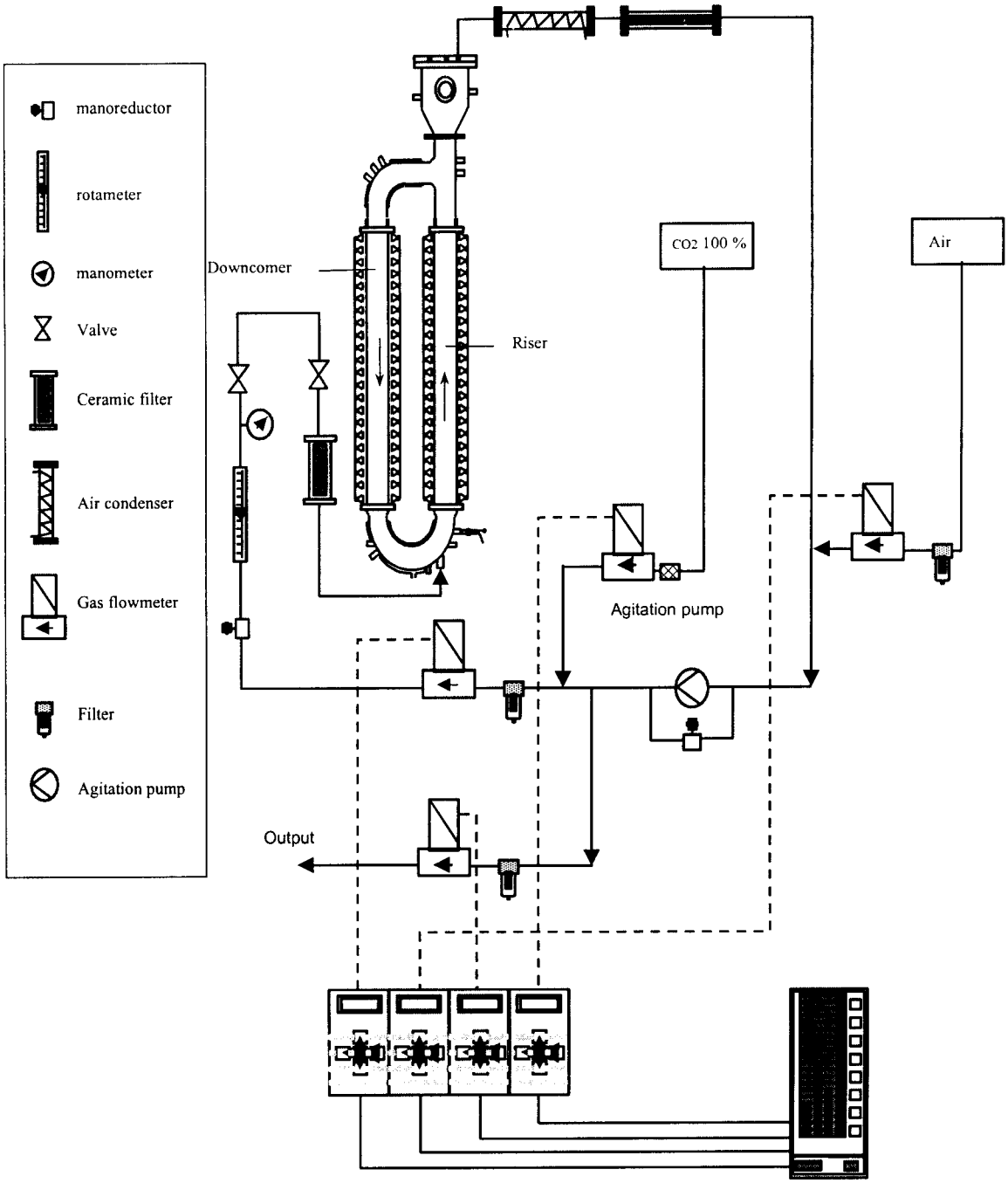

Figure 2: General scheme of the gas loop.

The mixing time in ALR is affected by the gas flow-rate, and therefore it is interesting to measure it for different aeration flows in the range available in the equipment. This will allow evaluation of the influence of the aeration and will help in the determination of the appropriate gas feed operational conditions.

When the reactor is operated in continuous culture conditions, the input-output flow is superimposed to the recirculation flow. As a consequence both factors will influence the residence time in the reactor. Not all the molecules entering the bioreactor at the same time will spend in it the same amount of time, due to the different possible paths along it. The characterisation of the mixing behaviour of a reactor is acomplished determining the residence time distribution (RTD) of its fluid elements (Levenspiel, 1972). This distribution results useful as a measurement of the non-ideal behaviour of the bioreactor, that is its deviation from the behaviour of an ideal reactor.

The usual technique for RTD determination is by injection of a tracer in the input of the bioreactor and to measure its concentration, respective to the input concentration, in the output along the time. The form of the obtained curve gives an information of the behaviour of the bioreactor.

Evaluation of the performance can be done by fitting mathematical models describing the hydrodynamic effects on that data. In those models, axial dispersion in the circulation flow is mainly modelled in two different ways. One way is as a combination of a series of stirred tank reactors, with the same volume each. Another way is using a diffusion model for different elemental processes, based each one on Fick's law of molecular diffusion, and adding them all in an effective longitudinal diffusion coefficient D_{eff}. The resulting diffusion model is characterised by the so called Bodenstein number (Bo) which is a measure of the relationship between mass transfer due to plug flow and that due to the superimposed longitudinal mixing (D_{eff}). The number of Bo has a direct relationship to the degree of mixing. If Bo is 0, mixing is complete. As Bo increases, the real flow approaches to the ideal plug flow behaviour. If Bo is bigger than 8 both types of models, diffusional and tank series, have a simple and direct correlation. One example of each of these two approximations has been used in the present study.

For the pulse-response tests, is of key importance the type of tracer used. In this work an acid pulse (HCl) was used for the mixing time tests, according to the method described by Verlaan (Verlaan et al 1989) using a 50 mM KCl solution as a mediun inside the reactor. This minimises the salt effect on to the properties of the air-water mixture and coalescence. With this method, air bubbles do not disturb the detection of the tracers by pH electrodes. This is in contrast to other kind of measures such as conductivity or absorbance. As a disadvantage, it presents that the pH response is not linear with the amount of tracer. This fact is taken into account by calibration of the amount of OH^- present at each pH for the KCl solution and using in the analysis, the calculated concentration of OH^- present. As an advantage to mention, the total amount of tracer needed to add to the ALR for the test, is two orders of magnitude lower than the one needed in other cases such as for conductivity measurements. The characteristics of the carbon dioxide equilibrium reactions and the effect that a small amount of tracer causes a strong change in pH effect make the pH range more suitable for measurements, the one between the 3.5-and 6.2 pH units. As can be seen in the results section, this method was used successfully in the determination of the mixing time tests. For the residence time tests, the HCl tracer was changed by a stained compound in order to have an direct visualisation of the mixing characteristics of the bioreactor.

In addition to the distribution of all the reaction components inside the bioreactor, which is characterised by flow, mixing and residence time, it is also equally important in this bioreactors, to evaluate the mass transfer between the gas and liquid phases. Indeed in the envisaged operation of the reactor, carbon dioxide has to be provided to the cells from the gas phase and the oxygen produced by the cells has to be removed.

Therefore the transfer of those compounds between the liquid phase and the gas phase is of key importance.

Any gas required by the cell has to be first dissolved in the culture medium and this implies that the gas molecules have to change phase from the gas to the liquid phase or *vice versa*. The usual theoretical approximation to this fact is done by assuming that the occurring steps taking place follow the 'film theory'. According to this theory, it is assumed that it exists a gas-liquid interface which creates discontinuity. For example in the case of gas transfer to the liquid phase, the gas molecules have to diffuse from the bulk of the gas to the interface. This step is affected by turbulence of the gas. Once at the gas-liquid interface the gas molecules have to cross it, which is assumed to take place assuming a constant equilibrium state according to Henry's law. After, the molecule diffuses from the gas-liquid interface into the bulk of liquid according to Fick's first law of diffusion. The combination of these facts affect the velocity of gas transfer per unit surface, and the limiting step in this process is usually the gas transfer across the liquid film around the interface. On the other hand the total interface surface available for transfer is also of key importance. For this reason the total number of 'bubbles' present in the bioreaction per unit time (gas hold up) and their distribution, have an important effect on its performance. The total amount of interface surface existing in the bioreactor is hardly ever known and its effects are taken into account together with the limiting step mass transfer coefficient in a lumped coefficient known as k_La. Experimental determination of this coefficient informs of the capacity of the bioreactor to supply a determined compound from the gas to the liquid phase or in the oposite sense for those compounds with drawn from the liquid to the gas phase.

EXPERIMENTAL TESTS.

Mixing time determination

Material and methods

Experimental determination of the mixing time was done according to the impulse response test using HCl as a tracer, as described by Verlaan (VERLAAN *et al* 1989).

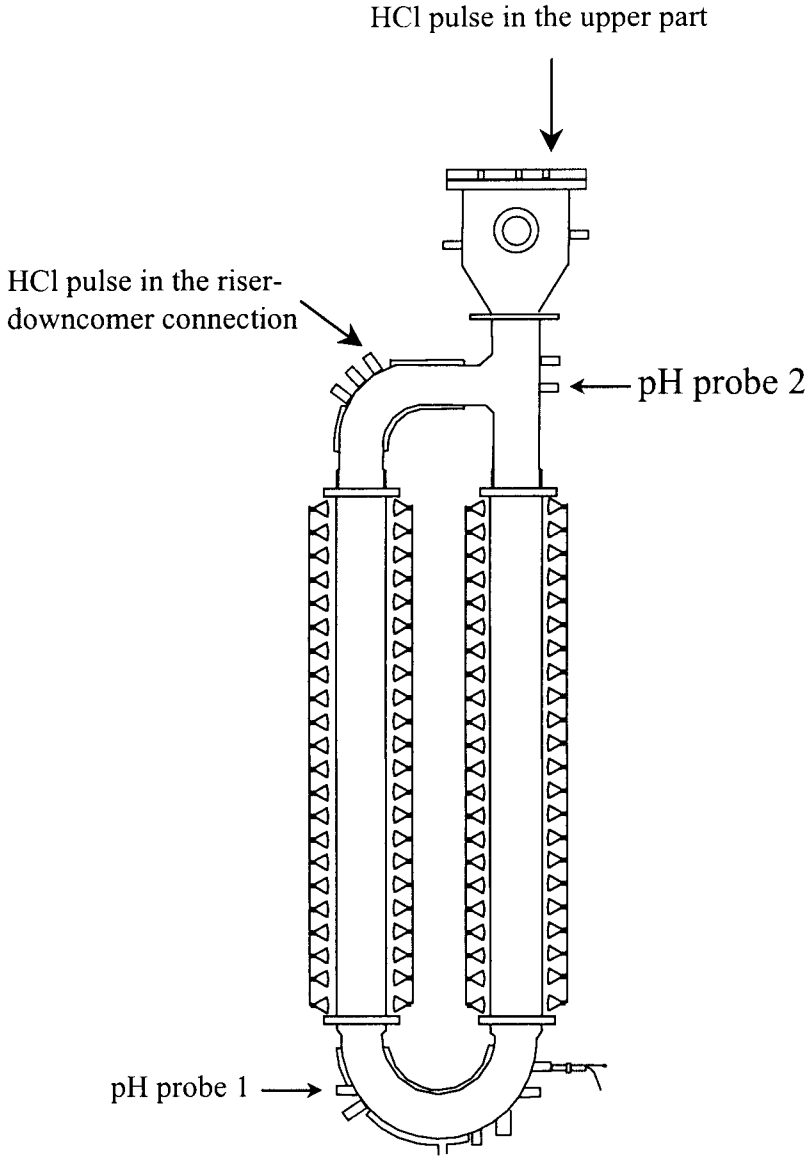

Figure 3: Position of the pH probes and injection points for the mixing time determination.

The gas-lift loop reactor was filled with a 50 mM KCl solution. At zero time, 1 ml of concentrated HCl was injected. Two pH probes were used to follow the evolution of the tracer concentration. The probes were located at the top of the riser and at the bottom of the downcomer (figure 3). The tracer was injected either on the top part of the reactor or at the entrance of the downcomer (see figure 3). The pH values were registered with a frequency of 2 seconds.

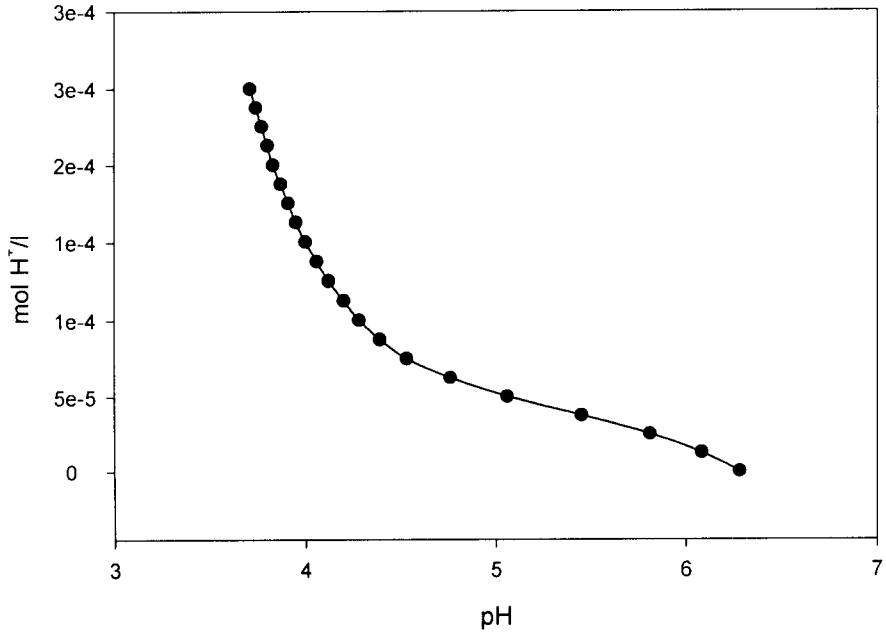

Figure 4: Calibration curve of ion concentration in function of pH, for a 50 mM potassium chloride solution.

Correction for the non-linearity of the tracer concentration in front of the pH was done by using a calibration curve. The calibration curve was performed by measuring the pH changes of a 50 mM KCl solution for different amounts of HCl added. The resulting curve (Figure 4) allowed to derive the following correction function:

$$C_t = 0.2033*10^{-4}*\mathrm{pH}^4 - 4.4734*10^{-4}*\mathrm{pH}^3 + 36.69*10^{-4}*\mathrm{pH}^2 - 0.013334*\mathrm{pH} + 0.0182$$
$$R = 0.9996 \qquad (1)$$

Dimensionless concentration for the ion concentration was calculated using the following function:

$$C = \frac{(C_t - C_0)}{(C_\infty - C_0)} \qquad (2)$$

Were C_t is the ion concentration at t time. C_0 is the initial ion concentration. C_∞ is the ion concentration a equilibrium.

Experiments are carried out at different inlet gas flow rates comprised between the minimal flow rate to ensure good fluid circulation and the maximal flow rate imposed by physical limitations of the reactor. At higher flow rates, The increase of pressure inside the gas-lift would cause a deformation of the polyamide foil.

Summary of operating conditions:

- Inlet gas flow rates tested : 0.6, 0.9, 1.2, 1.3 and 4.5 l/min
- Liquid flow rate: none
- Gas loop: closed
-Temperature: 25 °C.

Mixing time experimental results and discussion.

Following the experimental conditions described in the previous section, several pulse response tests were performed. As described in table 1 each test was done at different airflow within the possible range in the reactor. Experimental conditions for each of the experiments conducted is provided in table 1.

Table 1: Summary of experimental tests done for mixing time evaluation.

Experiment N°	Inlet gas flow rate (ml/min)	Injection point
1	0.6	Connection riser/downcomer
2	0.9	Connection riser/downcomer
3	1.2	Upper part
4	1.3	Connection riser/downcomer
5	1.5	Connection riser/downcomer
6	4.5	Connection riser/downcomer

Results recorded for each experimental test, are plotted in figures 4 to 9. For each plot, ion concentration, calculated according to 'materials and methods' section, is represented with respect to time.

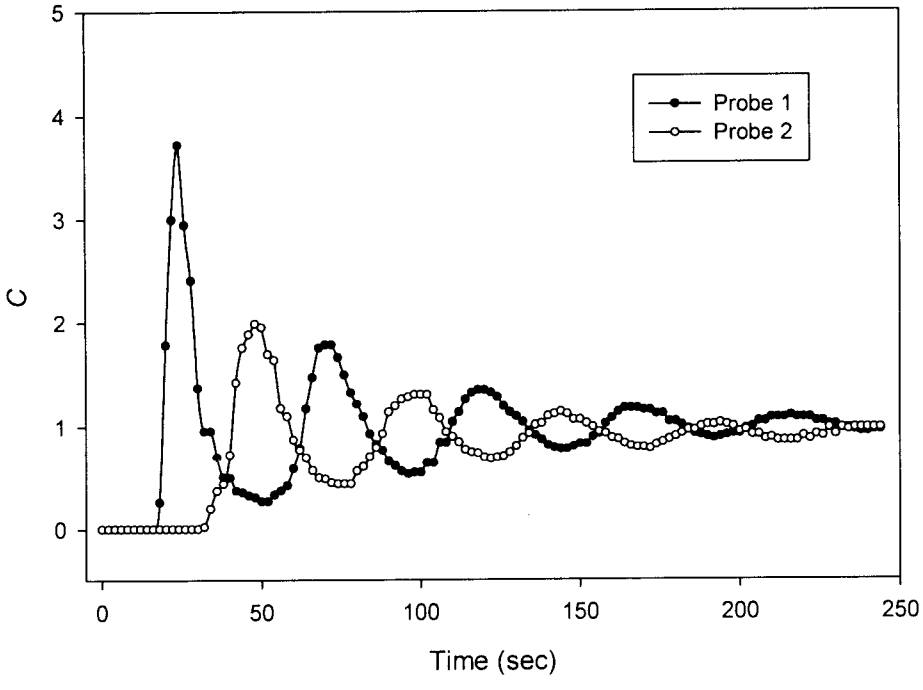

Figure 5: Normalised ion concentration evolution, as measured by the two pH probes, *versus* time during experiment 1.

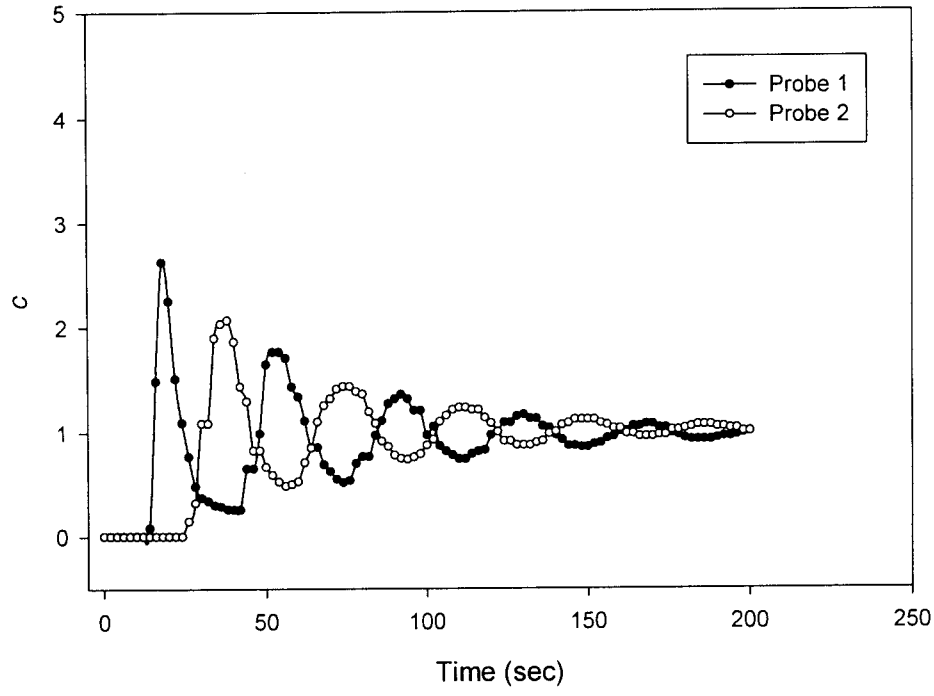

Figure 6: Normalised ion concentration evolution, as measured by the two pH probes, *versus* time during experiment 2.

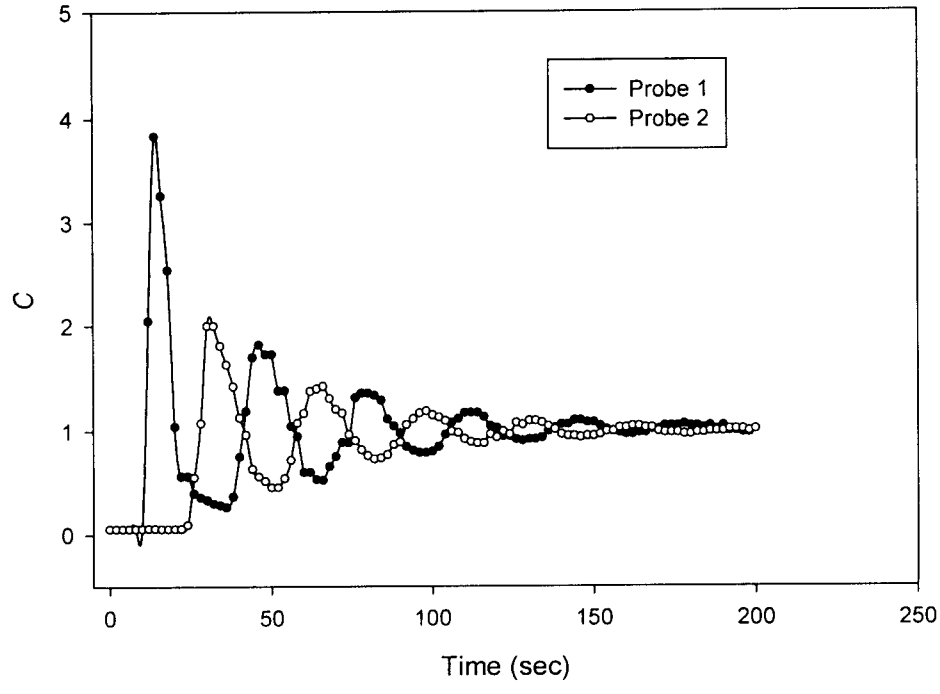

Figure 7: Normalised ion concentration evolution, as measured by the two pH probes, *versus* time during experiment 3.

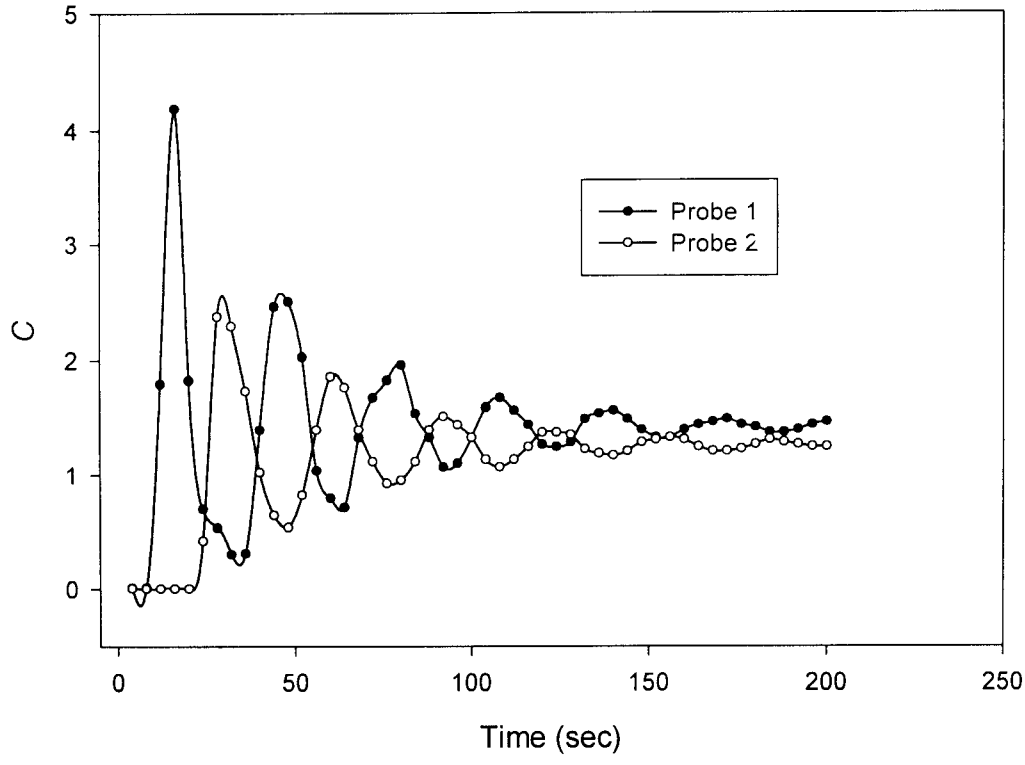

Figure 8: Normalised ion concentration evolution, as measured by the two pH probes, *versus* time during experiment 4.

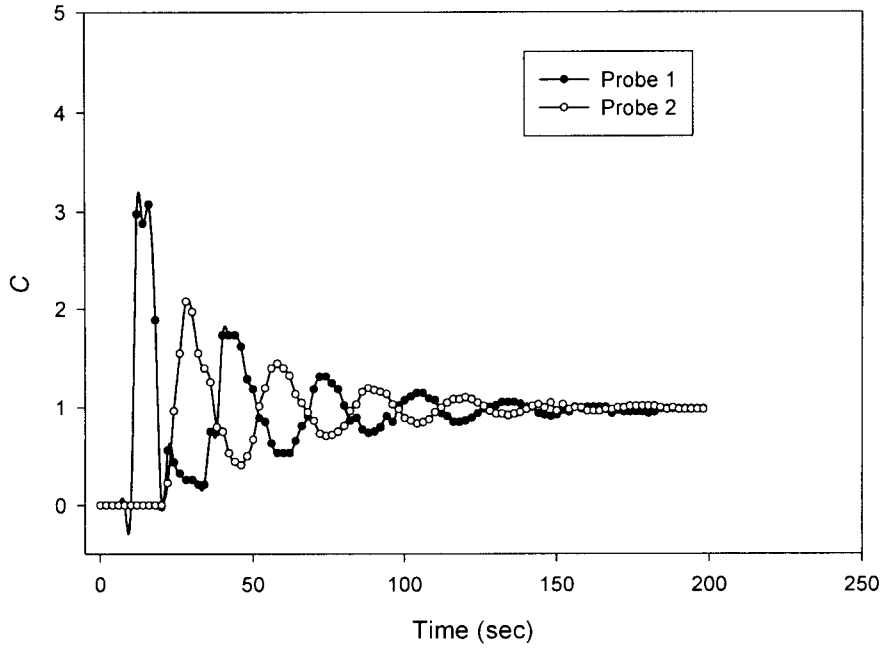

Figure 9: Normalised ion concentration evolution, as measured by the two pH probes, *versus* time during experiment 5.

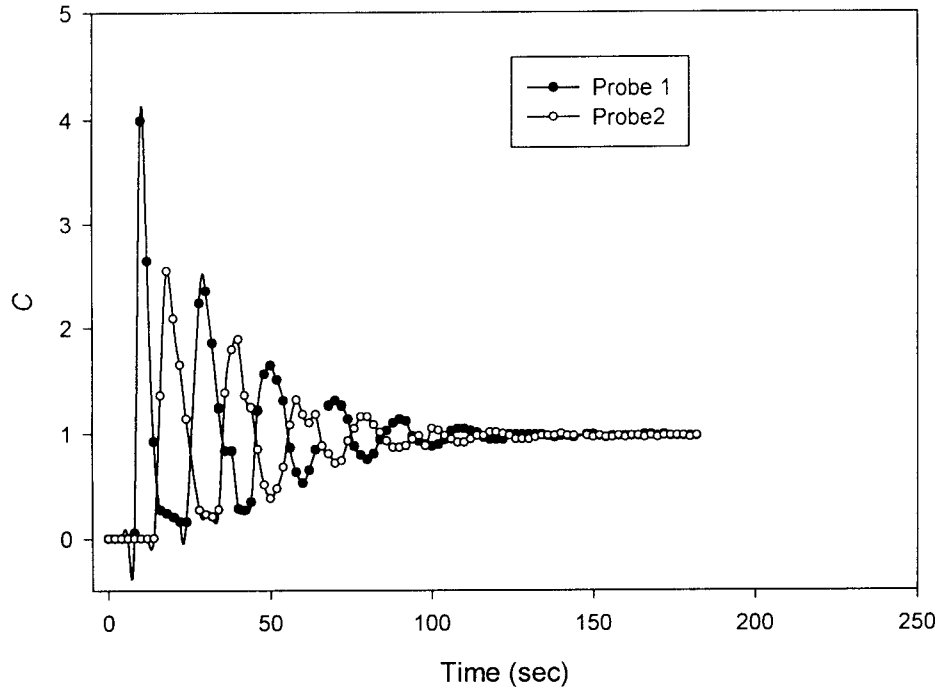

Figure 10: Normalised ion concentration evolution, as measured by the two pH probes, *versus* time during experiment 6.

All the curves present the same type of profile. The normalised ion concentration presents a damped oscillation, which decreases in intensity towards an equilibrium point. This point represents the ion concentration when it is completely and uniformly mixed inside the bioreactor. The amplitude of the pulse decreases exponentially while the frequency is constant.

The oscillation of the tracer concentration, can be explained by the circulation of the fluid in the gas-lift loop. Therefore, the oscillation frequency is related to the mean circulation velocity, while the damping of the oscillation is caused by the dispersion of the ion concentration in the liquid volume in the bioreactor. The changes in ion concentration appear earlier in the downcomer than in the riser, due to the direction of liquid circulation flow, and the location of the tracer injection point.

Circulation time and mixing time

Circulation time, that is the time required for the liquid to revolve one turn around the riser-downcomer loop, can be estimated from the time period between two adjacent peaks of the tracer response curves.

For the mixing time determination, it is necessary to previously define the degree of mixing which is usually characterised by defining the inhomogeneity of the fluid. The inhomogeneity (h) is defined as :

$$h = \frac{C - C\infty}{C\infty} \qquad (3)$$

Therefore mixing time can be defined as the time to reach a inhomogeneity of 5 %. This is convenient when the measure oscillates around an average value and indicates that the bioreactor has reached a 95% homogeneity. Following those definitions, mixing time and circulation time were calculated for the previously shown experiments (figures 5 to 10). Calculated results can be found in table 2.

Experiment N°	Inlet gas flow rate (ml/min)	Circulation time (s)	Mixing time (s)
1	0.6	50	242
2	0.9	38	157
3	1.2	32	152
4	1.3	32	138
5	1.5	30	139
6	4.5	20	117

Table 2: Summary of the circulation time and mixing time obtained for different inlet gas flow rates.

The results show that circulation time decreases proportionally to the increase of inlet gas flow rate. The values calculated were identical for the two locations of the pH probes.

On the other hand, mixing time decreases with increasing inlet gas flow rate and approach a constant value at higher gas flow rates. Calculation of mixing time in the downcomer gives lightly smaller values than in the riser because the probe is located nearer the injection point in the downcomer than in the riser.

Modelling of the bioreactor hydrodynamics.

In order to characterise the liquid flow behaviour of the bioreactor in the riser and the downcomer at the previously mentioned flow rates, two different mathematical models have been used, the axial dispersion model, and the tanks-in-series model.

Axial dispersion model

The fluid dispersion model used in this case was the same used in Verlaan (VERLAAN *et al.* 1989), according to the following equation:

$$C\theta = \left(\frac{Bo}{4\pi\theta}\right)^{1/2} \sum_{x=1}^{\infty} \exp\left[\frac{-(x-\theta)^2 Bo}{4\theta}\right] \qquad (4)$$

Where θ is the dimensionless time (θ = t/circulation time). x is the axial coordinate and Bo is the Bodenstein number : Bo= (ν*L) / D.

ν = liquid velocity (m/s)

L = lenght (m)

D= dispersion coefficient (m^2/s)

An example of the fitting results obtained is shown in figures 10 and 11, in which the above model is fitted to the signal obtained from the two probes for experiment 2.

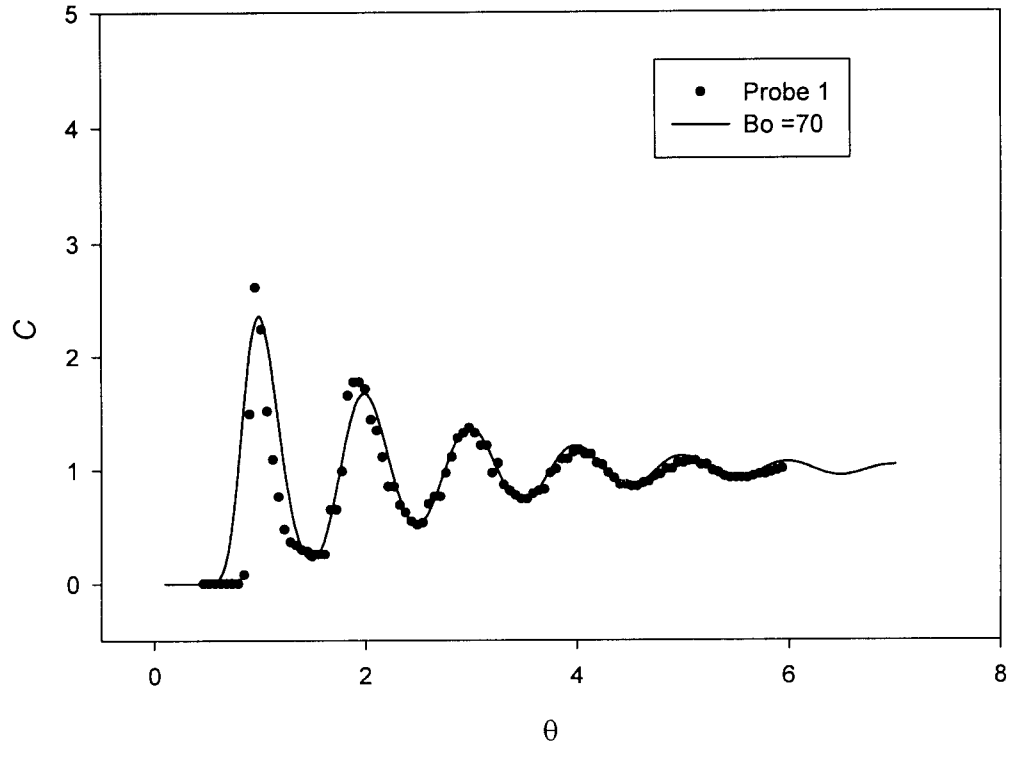

Figure 11: Results of the fitting of the dispersion model to the downcomer signal for experiment 2.

In all the cases, the best fitting between experimental and theoretical values and the model equation provided the corresponding Bo. For the pH probe located in the bottom of the riser, the first peak was not taken into account. However, model represents the rest of the peaks with high accuracy.

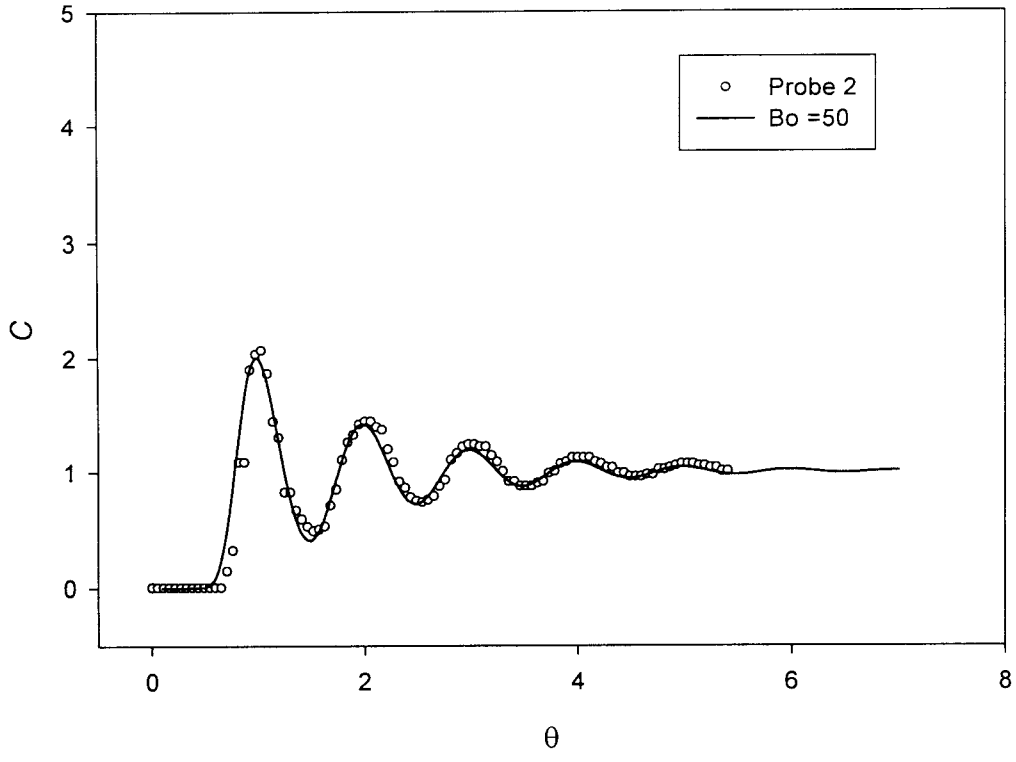

Figure 12: Results of the fitting of the dispersion model to the riser signal for experiment 2.

The Bo values obtained for the gas-lift reactor were 49 for the riser and 70 for the downcomer respectively. The downcomer shows the highest Bodenstein number due to the single-phase flow in this part, that is, barely no gas phase, which induces a lower dispersion. The Bodenstein (Bo) number values, that best allowed to fit the model to the experimental data, were the same for the different flow rates values tested.

This results are consistent with theoretical knowledge, which states that a higher Bo number is the result of a higher plug flow behaviour, while when the Bo number decreases it approximates more to the case were there is a higher degree of mixing.

Tanks in series model

The longitudinal mixing effect can also be represented using the tanks in series models. The equation of the model is :

$$C\theta = Ne^{-N\theta}\sum_{m=11}^{\infty}\exp\left[\frac{(N\theta)^{mN-1}}{(mN-1)!}\right] \qquad (5)$$

Where θ is the time, N is the number of tanks and m is the number of times the fluid recirculates.

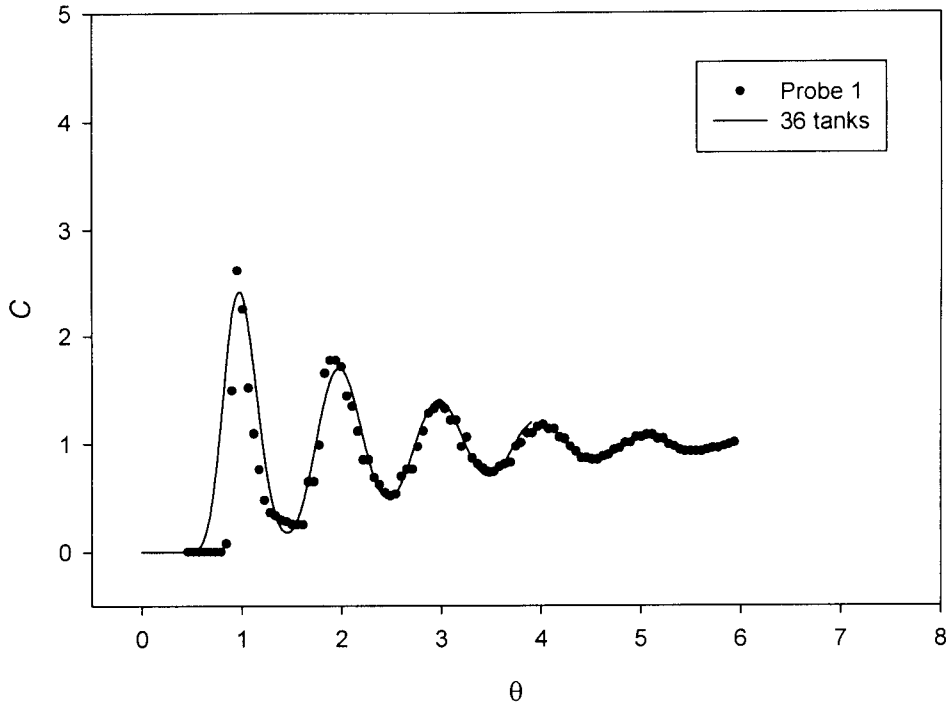

Figure 13: Results of the fitting of the tanks in series model to the riser signal for experiment 2

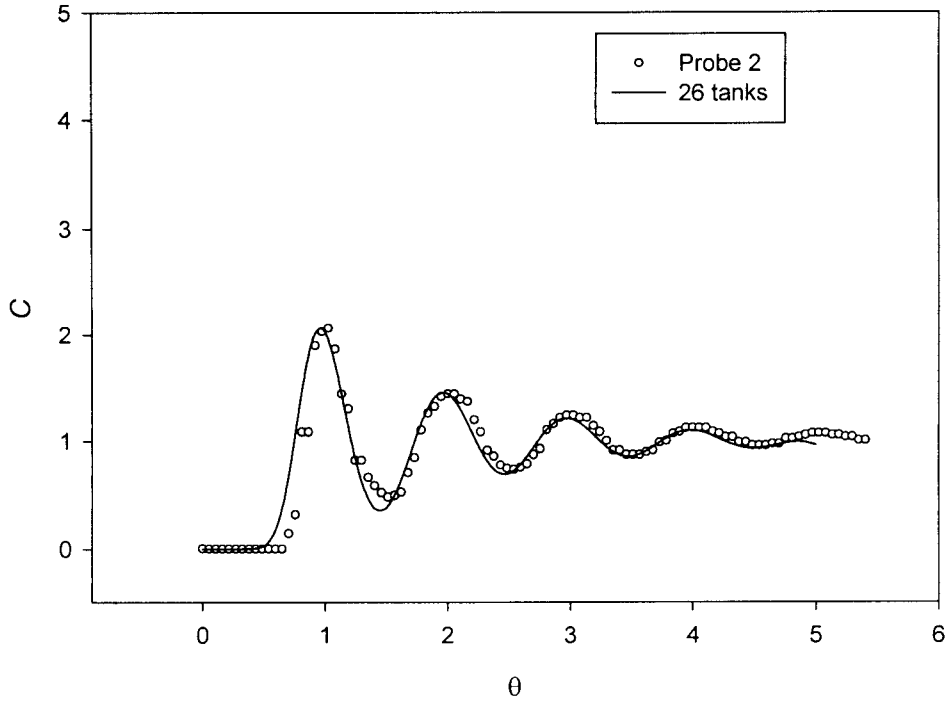

Figure 14: Results of the fitting of the tanks in series model to the downcomer signal for experiment 2

According to the results in figures 13 and 14, the riser and downcomer section behaviour can be simulated by using a model with 26 and 36 CSTR respectively. These results are in good accordance with the correlation of Blenke (BLENKE 1979) which reads as follows:

$$n = 1+Bo/2. \qquad (6)$$

Where n is the number of tanks in series and allows to compare the results of the two models.

Residence time distribution tests

Materials and methods.

In order to determine the residence time distribution, the reactor was operated in continuous mode, and a liquid flow was superimposed to the circulation flow of the system.

For the pulse response test, a colorimetric method was used and bright red acid 'duasyn' 4 RC (Hoechst) was chosen as a tracer. The optical density at 507 nm was measured and then converted to tracer concentration using a calibration curve of absorbance as a function of bright red concentration, previously obtained. An example of the calibration curve can be seen in figure 14. From the obtained calibration curve the following relationship among absorbance and tracer concentration was obtained:

$$C = 0.0316 * Abs - 0.0001 \qquad R = 0.9999 \qquad (7)$$

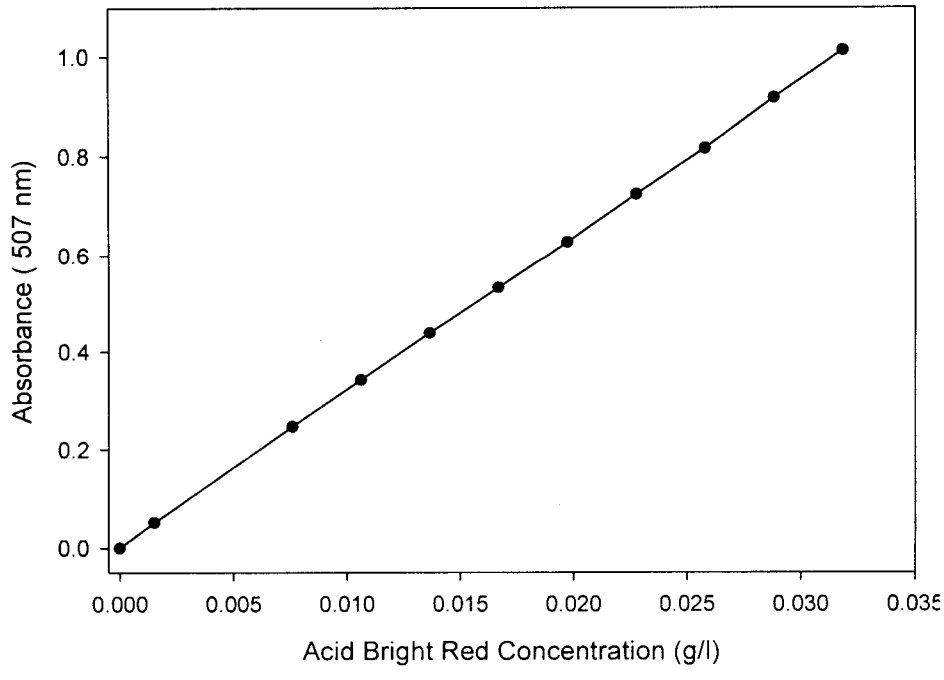

Figure 15: Calibration curve for acid bright red concentration.

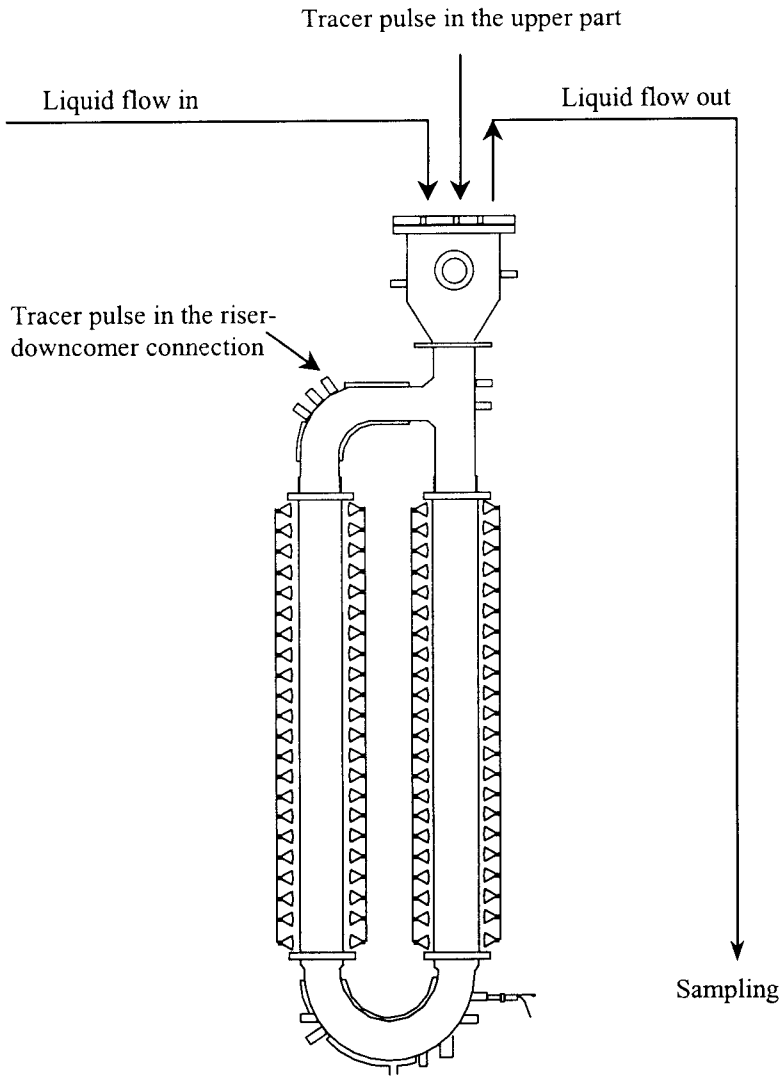

Figure 16: Tracer injection and sampling points for the RTD tests.

The pulse of tracer was injected either in the head of the reactor (experiment 1) or in the upper part of the riser-downcomer connection (experiment 2). Injection points are represented on figure 16. Samples were taken at the outlet of the reactor.

Other operating or conditions were:

(1) Gas loop: closed

(2) Gas flow rate: 1.2 l/min

(3) Liquid flow rate: 2.8 l/h

Residence time determination:

The following equation, obtained directly from a mass balance for the tracer in a CSTR reactor, is applied to determine the experimental mean residence time:

$$C = C_0 \exp\left(-\frac{t}{\bar{t}}\right) \tag{8}$$

Then, the parameter evaluation is done by least-squares curve fitting, based on the minimisation of the sum of squares of the differences between the experimentally measured response curve and the plot obtained by the following linearized flux model:

$$\ln C = \ln C_0 - \frac{t}{\bar{t}} \qquad (9)$$

Were 'C' is tracer concentration, 'C_O' is the initial tracer concentration after pulse introduction and $\bar{t}$ is the residence time.

Normalised curves were obtained by using the following adimensional variables:

$$\theta = \frac{t}{\bar{t}} \qquad (10)$$

$$E_\theta = (liquid\ \ flow) * \frac{[tracer\ \ concentration]}{quantity\ \ of\ \ tracer\ \ injected} * \bar{t} \qquad (11)$$

Normalised curve fitting was done representing E as a function of adimensional time (θ).

Residence time distribution results.

Experimental results for the normalised flux profiles and determination of the mean residence time distribution by linearization of the flux model equation are presented in figure 17, 18, 19 and 20.

Theoretical calculated residence time was of 27.5 hours and the experimental ones were of 28.08 and 28.32 hours for experiment 1 and experiment 2 respectively.

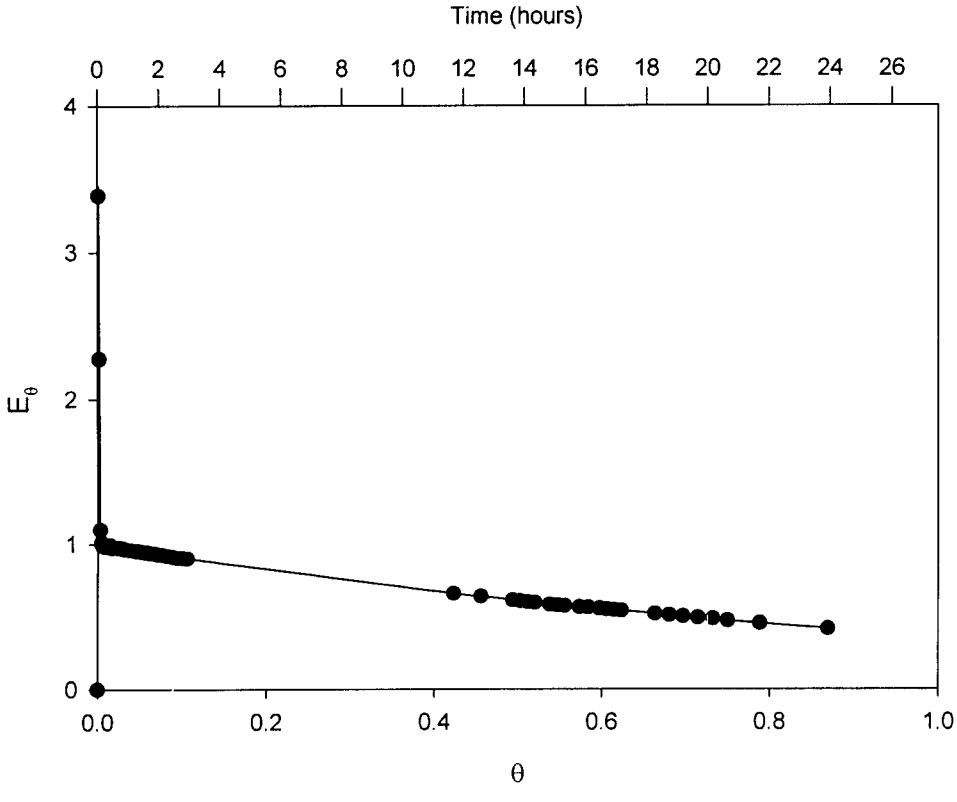

Figure 17: Experimental results for the RTD corresponding to experiment 1.

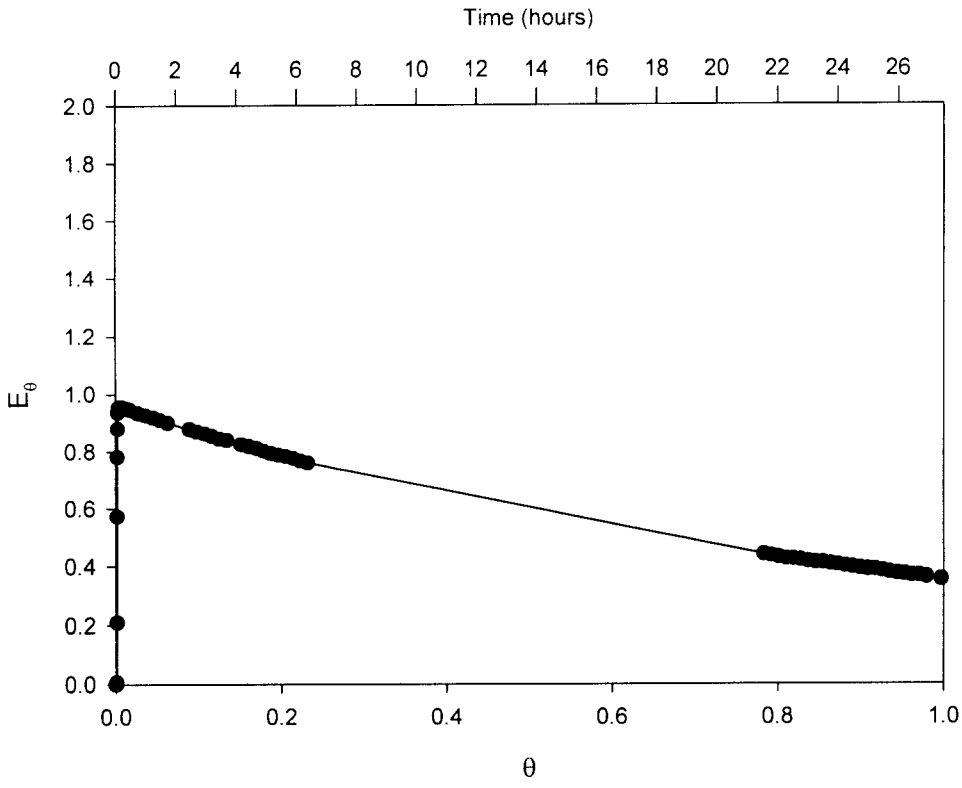

Figure 18: Experimental results for the RTD corresponding to experiment 2.

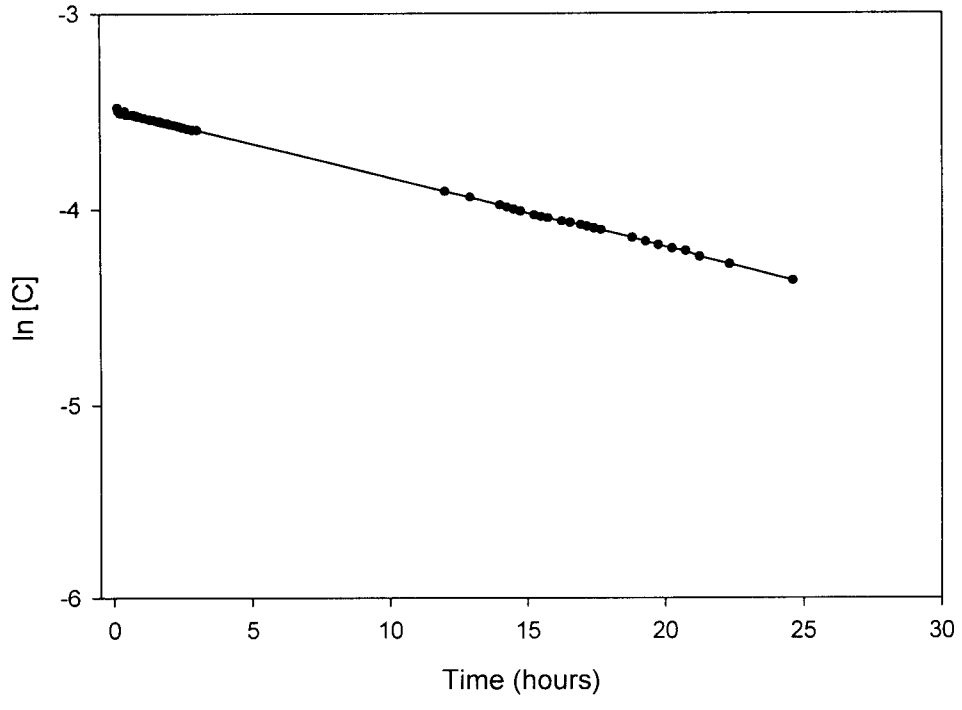

Figure 19: Linearization of the experimental results for the RTD corresponding to experiment 1.

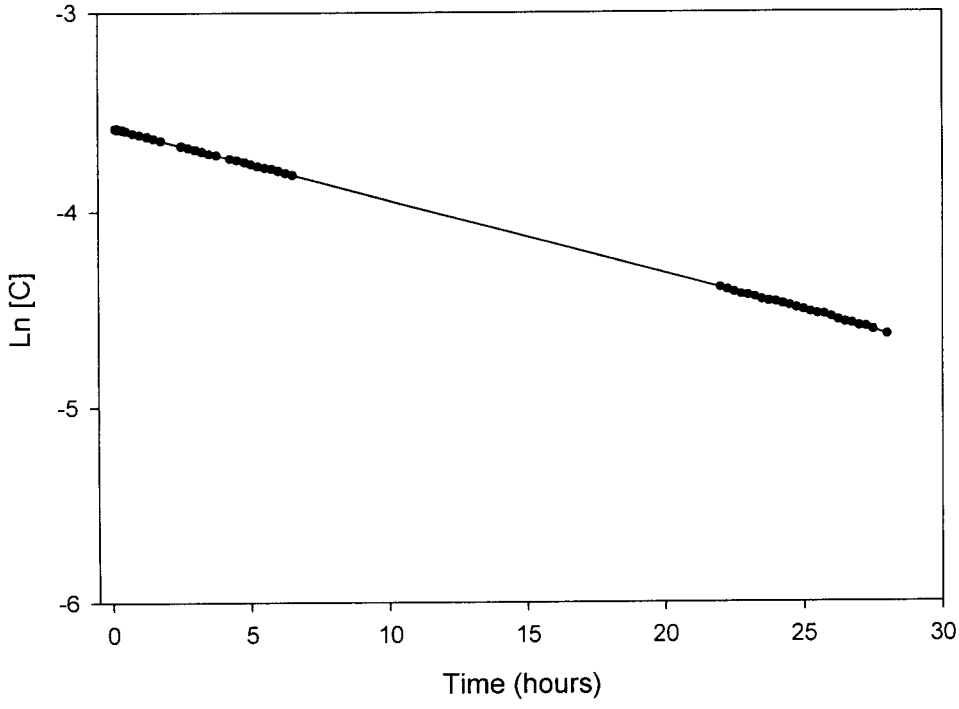

Figure 20: Linearization of experimental results for the RTD corresponding to experiment 2.

Figures 17 and 18 show the concentration profiles obtained in the outlet of the reactor after injection of the colorant in the upper part of the gas-lift reactor. Linearization results are shown in figures 19 and 20.

As the time scale is high, the reactor has the same behaviour than a CSTR. If the frequency of sampling at the beginning of the experiment would have been higher and the distance between the outlet of the reactor and the sampling location shorter, the effect of loop circulation would be traduced by oscillations in the tracer concentration profile.

In the case of experiment 1, the inlet of liquid and the outlet are very close. The high tracer concentrations measured in the first samples indicate a strong bypass effect. When the tracer injection point was more separated from the outlet of the reactor (experiment 2), no bypass effect was observed. Hence, for further continuous operation of the reactor, the inlet of culture medium should be done at a sufficient distance from the outlet.

Bioreactor $K_L a$ determinations

As mentioned in the introduction, measurement of the gas-liquid mass transfer coefficients under different operating conditions, is a key point in the evaluation of the performance of a bioreactor. Due to the nature of the bioreaction taking place in this bioreactor, the volumetric mass transfer coefficients for CO_2 and O_2 are the ones required. These two coefficients are numerically very close and the difference is in the order of the accuracy of the measurement. On the other hand, the fact that there is an equilibrium between the carbon dioxide (CO_2), carbonate (CO_3^{2-}) and bicarbonate (HCO_3^-) carbon species, implies that the usual assumption of non accumulation of dissolved gasses inside the medium, which is the classical approach, is no longer valid. This imposes and added factor of complexity on the calculation of the CO_2 mass transfer coefficient which is bound to result in a lower precision of the determination. Therefore, for this reasons, in the present work it will be assumed that the two coefficients are numerically equivalent for the two cases, as in Technical Note 32.4 (CORNET 1998). Therefore only the O_2 mass transfer coefficient was determined, as it is the easier determination to carry out experimentally.

Materials and methods.

For the volumetric oxygen mass transfer coefficient ($K_L a$), the dynamic method was used. As the dynamics of the oxygen electrode may influence the $K_L a$ results, its response time was determined by submerging it alternatively in two vessels, one sparged with air and another one with nitrogen gas. This way the response time can be determined.

The electrode signal, S(t), is supposed to be first-order time dependant following:

$$\frac{dCmed}{dt} = \frac{(C - Cmed)}{\tau} \qquad (12)$$

From this equation, the time constant was obtained as the time necessary to reach 63.2 % of the response. Figure 21 shows the response of the probe after a change from the nitrogen-sparged vessel to the oxygen-sparged one.

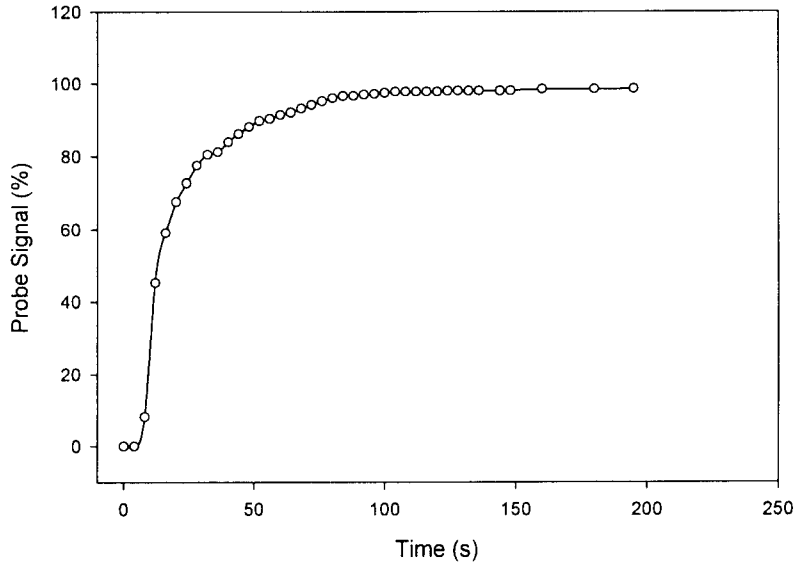

Figure 21: Time response of the probe signal for the response time determination.

For the determination of K_L**a**, the oxygen concentration in aqueous liquid phase inside the reactor was measured and monitored as a function of time, after a step change in the supplied gas from nitrogen to air.

The dissolved oxygen values were measured by an oxygen probe located either in the upper part of the riser or in the lower part of the downcomer and monitored by a Mettler 4500 O_2 transmitter. The rate of oxygen absorption is given by:

$$\frac{dC}{dt} = K_L a * (C^* - C) \qquad (13)$$

Where C* is the oxygen concentration in gas-liquid interphase at equilibrium with the gas concentration. A combination of equation 12 and equation 13 and integration gives the theoretical signal at time t:

$$Cmed = \frac{C^*(1-\exp(-K_L a * t) - K_L a * t(1-\exp(-\frac{t}{\tau})))}{1 - K_L a * \tau} \qquad (14)$$

K_La can thus be evaluated by fitting equation 14 to the experimentally measured electrode signal.

K_La experimental results

Following the method described in the previous section, the K_La was determined for different aeration flow rates of the bioreactor and different positions of the oxygen probe. An example of the K_La determination is presented in figure 22. The experimental values obtained show an evolution according to the expected values, and allow for an appropriate fitting of equation 13 and determination of the K_La. The obtained values are in good agreement with the values that can be expected for this kind of bioreactor and conditions. The obtained results are summarised in table 3.

Experiment N°	Inlet gas flow rate (ml/min)	Injection point	$K_L a^{36°C}$ value (h^{-1})
1	1.2	Upper part of the reactor	6.0
2	2.1	Upper part of the reactor	8.8
3	3.0	Upper part of the reactor	11.2
4	4.5	Upper part of the reactor	15.4
5	1.2	Bottom of the downcomer	7.3
6	3.0	Bottom of the downcomer	12.0
7	4.5	Bottom of the downcomer	14.7

Table 3: Determined K_La values for the different experimental conditions.

The obtained results indicate that K_La is highly sensitive to the gas flow rate and the K_La coefficients increase with increasing inlet gas flow rate, as could be expected. However in all of the cases, K_La values obtained are slightly lower than the ones obtained by Cornet (CORNET 1998), in the working conditions adequate for this bioreactor. To reach a K_La value similar to the values obtained by Cornet, an inlet gas

flow of 4.5 l/min has to be used. However, the K_La increase by using higher gas flows rates is limited by the physical characteristics of the reactor construction materials. Indeed, as the gas flow is increased, inlet pressure in the reactor increases and the plastic foil of the illuminated volume swells after reaching a certain value. This deformation can induce important changes in the liquid volume in the reactor.

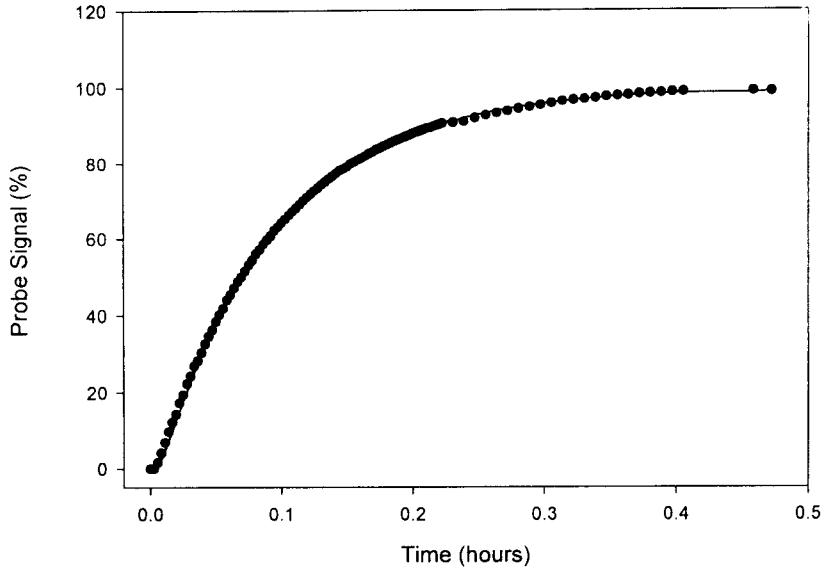

Figure 22: Oxygen probe response during one of the K_La determination tests.

Improvement of K_La is not the only way of achieving better gas transfer performance. The increase of the CO_2 or O_2 transfer driving force (C^*-C_L) is an alternative to the enhancement of CO_2 or O_2 mass transfer. C^* can be increased by increasing the gas mole fraction of O_2 or CO_2 in the inlet of the reactor, allowing this way to reach the same gas transfer performance. Nevertheless application of this possibility is also related to the gas consumption/production capabilities of the strain cultured, and will have to be evaluated under real culture conditions using the *Spirulina* strain.

REFERENCES

BLENKE H. (1979) Loop Reactors. Adv. Biochem. Bioeng.13:121-214.

CORNET J.F.; MARTY A.; DUSSAP G.; (1988) Analysis of Carbon Limitation in the *Spirulina* Compartment.

LEVENSPIEL O. (1972) Chemical Reaction Engineering, 2nd ed., Wiley, New York.

VERLAAN, P.; VAN EIJS A.M.M.; TRAMPER J.; VAN'T RIET LUYBEN K.CH.A.M. (1989) Estimation of Axial Dispersion in Individual Sections of an Gas-lift-Loop Reactor. Chemical Engineering Science 44:1139-1146.

VERNEREY A.; ALBIOL J.; GODIA F. (1996) Photosynthetic Pilot Reactor. TN 25.2 ESTEC/CONTRACT 11549/95/N2/FG.

VERNEREY A.; ALBIOL J.; GODIA F. (1998) Set up of Pnotosynthetic Pilot Reactor. TN 37.2 ESTEC/CONTRACT 11549/95/N2/FG.